The Astrophysical Journal Supplement Series, 154:147–150, 2004 September

THE FAR- AND MID-INFRARED/RADIO CORRELATIONS IN THE *SPITZER* EXTRAGALACTIC FIRST LOOK SURVEY

P. N. Appleton,[1] D. T. Fadda,[1] F. R. Marleau,[1] D. T. Frayer,[1] G. Helou,[1] J. J. Condon,[2] P. I. Choi,[1] L. Yan,[1] M. Lacy,[1] G. Wilson,[1] L. Armus,[1] S. C. Chapman,[3] F. Fang,[1] I. Heinrichson,[1] M. Im,[4] B. T. Jannuzi,[5] L. J. Storrie-Lombardi,[1] D. Shupe,[1] B. T. Soifer,[1] G. Squires,[1] and H. I. Teplitz[1]

Received 2004 March 27; accepted 2004 May 5

ABSTRACT

Using the *Spitzer Space Telescope* and the Very Large Array (VLA), we present the first *direct* evidence that the well-known far-infrared/radio correlation is valid to cosmologically significant redshift. We also confirm, with improved statistics compared with previous surveys, a similar result for the mid-IR/radio correlation. We explore the dependence of monochromatic q_{24} and q_{70} on z. The results were obtained by matching *Spitzer* sources at 24 and 70 μm with VLA 1.4 GHz microjansky radio sources obtained for the *Spitzer* First Look Survey (FLS). Spectroscopic redshifts have been obtained for over 500 matched IR/radio sources using observations at WIYN and Keck, and archival Sloan Digital Sky Survey (SDSS) data extending out to $z > 2$. We find that q_{24} shows significantly more dispersion than q_{70}. By comparing the observed fluxes at 70, 24, and 4.5 μm with a library of SED templates, we find that the larger dispersion in q_{24} is predictable in terms of systematic variations in spectral energy distribution (SED) shape throughout the population. Although the models are not able to encompass the full range of observed behavior (both the presence of either extremely flat or extremely steep IR SEDs), the fitting parameters were used to "k-correct" the higher z galaxies, which resulted in a reduced scatter in q. For comparison, we also corrected these data using the SED for M82. The results for 24 and 70 μm provide strong consistent evidence for the universality of the mid- and far-IR/radio correlations out to redshifts of at least $z = 1$.

Subject headings: cosmology: observations — galaxies: evolution — galaxies: high-redshift — infrared: galaxies

1. INTRODUCTION

It has now been more than a quarter of a century since the first hints emerged of a very tight correlation between the global far-infrared (FIR) and radio emission from galaxies. Initially based on comparisons between challenging ground-based 10 μm/radio correlations of small samples of galaxies (van der Kruit 1973; Condon et al. 1982; Rickard & Harvey 1984), the remarkable nature of the FIR/radio correlation became increasingly apparent with larger IR samples obtained from the *Infrared Astronomical Satellite* (*IRAS*) All Sky Survey (Dickey & Salpeter 1984; de Jong et al. 1985; Helou et al. 1985; Condon & Broderick 1986; Wunderlich et al. 1987; Hummel et al. 1988; Fitt et al. 1988). *IRAS* showed that the FIR/radio correlation appeared to apply to a wide range of Hubble types extending over more than 3 orders of magnitude in IR luminosity from dust-rich dwarfs to ultraluminous infrared galaxies (ULIRGs).

Although revolutionary, *IRAS* could only systematically study the relatively nearby universe. The *Infrared Space Observatory* (*ISO*) probed, for the first time, galaxy populations in the higher-z universe, but had limited long-wavelength coverage and sensitivity. Based on the deepest *ISO* fields, it was evident that even at 15 μm there was a loose correlation between the mid-IR (MIR) emission and the radio continuum (Cohen et al. 2000; Elbaz et al. 2002; Gruppioni et al. 2003). Using M82 as a template, Garrett (2002) extrapolated from 15 μm to longer wavelengths and suggested that the FIR/radio correlation probably extends to $z > 1$. At the other extreme, submillimeter observations using instruments like SCUBA began to reveal a new population of likely star-forming active galaxies. Although the statistics and redshift determinations are still growing (see Chapman et al. 2003), the correlation between microjansky radio and SCUBA sources suggest that the FIR/radio correlation is likely to be valid at much higher redshift (see Carilli & Yun 1999; Ivison et al. 1998, 2002; Frayer et al. 1999). The universality of the correlation, if confirmed, is important because it implies that galaxies observed at large look-back times share many of the same properties as fully formed mature galaxies seen locally.

2. *SPITZER* AND VLA RADIO AND SPECTROSCOPY OBSERVATIONS

Spitzer observations[6] of the First Look Survey (FLS) were obtained from 2003 December 1–11 (L. Storrie-Lombardi et al. 2004, in preparation; Fadda et al. 2004). A total of 4 deg^2 were covered by both the Infrared Array Camera (IRAC; 3.6, 4.5, 5.8, 8.0 μm; Fazio et al. 2004) and Multiband Imaging Photometer for *Spitzer* (MIPS; 24, 70, and 160 μm; Rieke et al. 2004) instruments at medium depth (5×12 s for IRAC,

[1] *Spitzer* Science Center, MC 220-6, California Institute of Technology, Pasadena, CA 91125; apple@ipac.caltech.edu.
[2] NRAO, 520 Edgemont Road, Charlottesville, VA 22903-2475.
[3] Department of Physics, California Institute of Technology, MC 320-47, Pasadena, CA 91125.
[4] Seoul National University, Shillim-dong, San 56-1, Kwanak-Gu, Seoul, South Korea.
[5] NOAO, 950 North Cherry Avenue, P.O. Box 26732, Tucson, AZ 85726.

[6] This work is based (in part) on observations made with the *Spitzer Space Telescope*, which is operated by the Jet Propulsion Laboratory, California Institute of Technology, under NASA contract 1407.

2×40 s for MIPS 24 μm, 1×40 s at 70 μm, and 2×4 s at 160 μm), and a smaller "verification strip" (0.25 deg^2) was observed to an even greater depth (4×40 s). The IRAC and MIPS 24 μm data were processed through standard *Spitzer* Science Center pipelines (M. Lacy et al. 2004, in preparation). The average FWHM of the point-spread function of the final maps were $\sim 2''$ for the IRAC bands and $6''$, $18''$, and $40''$ for MIPS 24, 70, and 160 μm, respectively.

IRAC sources were extracted (M. Lacy et al. 2004, in preparation) using the package SExtractor (Bertin & Arnouts 1996). MIPS 24 and 70 μm sources were extracted from the images using the StarFinder method (Diolaiti et al. 2000). The formal 5 σ sensitivities are measured to be 6, 7, 45, and 32 μJy for IRAC (3.6, 4.5, 5.8, and 8 μm, respectively) and 0.3, 30, and 100 mJy for MIPS (24, 70, and 160 μm, respectively). Tests performed on data from both the full survey and the verification strip at 24 and 70 μm indicate that the source flux densities show good reliability and repeatability down to a flux density of $\sim$0.5 and 30 mJy, respectively.

Radio observations were carried out by Condon et al. (2003) down to a formal 5 σ depth of 115 mJy with 35 overlapping *B*-array VLA pointings (FWHM of restored synthesized beam of $5''$), revealing over 3500 microjansky radio sources. This conservative limit is appropriate for the entire survey, including the edges of the field which were not surveyed as deeply as the inner regions. Given the coverage of the MIPS and IRAC fields, which did not extend to the outer edges of the VLA survey, we used a slightly deeper catalog ($S_{20\,\mathrm{cm}} > 90$ μJy prepared by J. J. C.) that was more appropriate for cross-matching with the *Spitzer* data. The deeper VLA catalog was found to provide a high degree of reliability when cross-correlated with deep *R*-band imaging of the same field.

Our sample consists of VLA radio sources with MIPS 24 and/or 70 μm counterparts and known spectroscopic redshifts. Source matching between the *Spitzer* and radio catalogs involved an automated catalog search followed by a visual inspection of the IR and radio images (this was important because of the possible presence of noise artifacts in the 70 μm images near the edges of scan legs). For the IRAC and MIPS 24 μm source catalogs, we searched for IR counterparts to VLA sources within a radius of $r < 2\farcs5$ of the VLA centroid. For the MIPS 70 μm images, the search was performed out to a radial distance of $12''$, because of the larger effective beam size of the 70 μm observations. For the MIPS 24 and 70 μm searches, 508 and 227 matched sources were found, respectively. Of the more than 3000 matched IRAC/VLA sources, 412 4.5 μm sources were in common with the MIPS/VLA sample used in this paper.[7] So few 160 μm detections were made that we restricted ourselves to the shorter wavelengths.

Spectroscopy of likely MIPS sources was performed before the launch of *Spitzer* by targeting VLA radio sources in two separate surveys. The first comprised $\sim$1200 radio sources that were observed using the NOAO-WIYN/Hydra fiber system (F. Marleau et al. 2004, in preparation), while the second survey yielded 80 radio sources targeted with the Keck II/Deimos spectrograph. The latter was part of a larger spectroscopy study of the FLS (P. Choi et al. 2004, in preparation). These data were supplemented with archival redshifts from the Sloan Digital Sky Survey.

3. MODEL-DEPENDENT "*K*-CORRECTIONS"

In this paper we present primarily flux-density ratios between the IR and the radio observations. Neglecting the $(1+z)^{-1}$ bandwidth compression term of the frequency units of flux density (Weedman 1986; Hogg et al. 2002), which cancels for flux ratios, the radio flux densities were boosted by a factor $(1+z)^{0.7}$, where we assumed a synchrotron power law of the form $S \propto \nu^{-0.7}$: a spectral index of +0.7, a value typical of an average steep-spectrum radio source. The boosting corrects the observed flux density at the emitted frequency to the value it would have at the observed frequency in its rest frame.

We approach the IR *k*-correction using two methods. Where 4.5, 24, and 70 μm data were available, we compared these data with a set of redshifted spectral energy distributions (SEDs) from Dale et al. (2001, hereafter DH01) and used these to compute the correction. As we shall see, the models only partly encompass the observed galaxy behavior. Therefore, as a second approach (and to extend the SED corrections to cover a larger number of 24 μm sources) we also use a complete SED for M82 (Fadda et al. 2002) appropriately convolved to the resolution of the *Spitzer* filters to correct these data.

The DH01 SEDs are a set of galaxy SEDs ranging from optical to submillimeter wavelengths and covering 64 different levels of excitation, as measured by the dust excitation parameter α ranging from 0.063 to 4.[8] As discussed in detail by DH01, values of α less than 1 correspond to a luminous starburst, while larger α values are more appropriate for describing quiescent systems. To select the best suited template SED, we computed the 4.5, 24, and 70 μm fluxes of each template redshifted to the value appropriate for each galaxy. We then use the observed 4.5, 24, and 70 μm flux densities (or 4.5 and 24 μm if 70 μm is unavailable) to perform a χ^2 fit to the *Spitzer* data. We selected the model that returned the lowest value of χ^2. The flux density at the observed frequency in the best-fitting model SED was then compared with the same frequency in the $z = 0$ model to derive the *k*-correction for that target galaxy.

4. FAR- AND MID-IR/RADIO CORRELATION AS A FUNCTION OF REDSHIFT

In Figure 1*a* we show the monochromatic 20 cm versus 70 μm luminosity correlation.[9] The plot shows that galaxies span 4 orders of magnitude in IR luminosity, and that a small number of radio-dominant active galactic nuclei (AGNs) are seen above the main trend. However, because of the distance-squared stretching of points in this diagram, we prefer to discuss the correlation and its dependence on redshift in terms of the more basic observable parameters–namely q_{IR}, where $q_{\mathrm{IR}} = \log(S_{\mathrm{IR}}/S_{20\,\mathrm{cm}})$ and S_{IR} is the flux density in the 24 or

[7] The reason we used IRAC 4.5 μm sources in this paper is because we have strong evidence in our sample that the 5.8 and 8.0 μm sources are strongly evolving in flux in the z range 0–0.8, presumably because of the shifting out of these bands of the 3.6, 6.2, and 7.7 μm infrared features. Using the 4.5 μm sources also increased the number of MIPS/VLA matches compared with the less sensitive IRAC filters at longer wavelengths

[8] The galaxy SEDs are created by combining individual "model" SEDs according to a power-law distribution in $UdM(U) \propto U^{-\alpha}\,dU$, where $M(U)$ represents the dust mass heated by radiation of energy density U.

[9] Here the emitted luminosity is $L_{\nu e} = 4\pi d_l^2 S_{\nu\mathrm{obs}}/(1+z)$ (Hogg et al. 2002), where $S_{\nu\mathrm{obs}}$ has already been *k*-corrected for an assumed SED as previously discussed. The luminosity distance d_l assumes $H_0 = 70$ km s^{-1} Mpc^{-1}, $\Omega_M = 0.3$, and $\Omega_\Lambda = 0.7$.

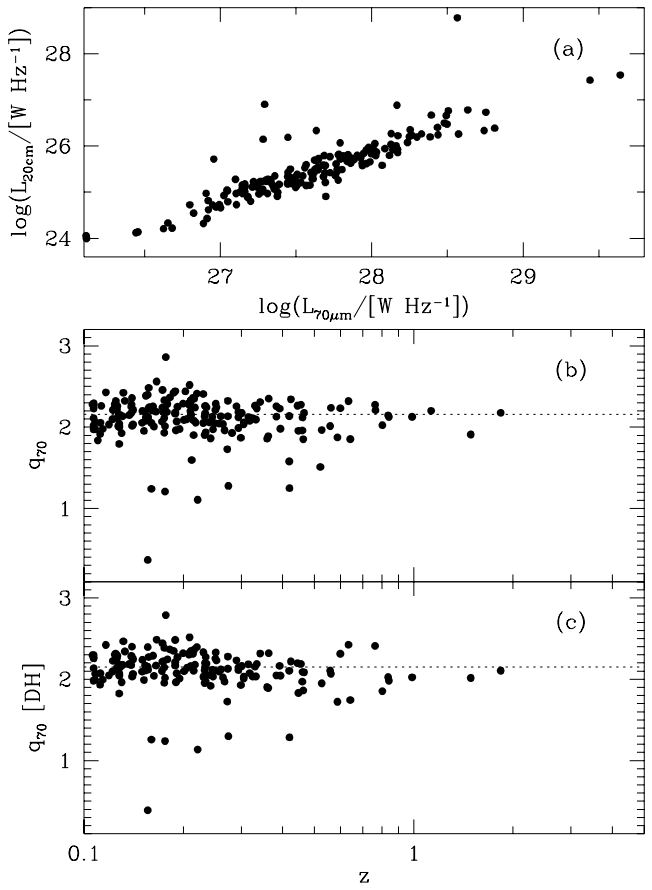

FIG. 1.—(*a*) 20 cm radio and 70 μm IR luminosity correlation (see text) for the FLS long-wavelength sample and the distribution of monochromatic q_{70}-values with redshift (*b*) uncorrected and (*c*) *k*-corrected using the DH01 SED-fitting method described in the text for the IR flux densities and assuming a $(1+z)^{0.7}$ *k*-corrected (boosting) of the 1.4 GHz values.

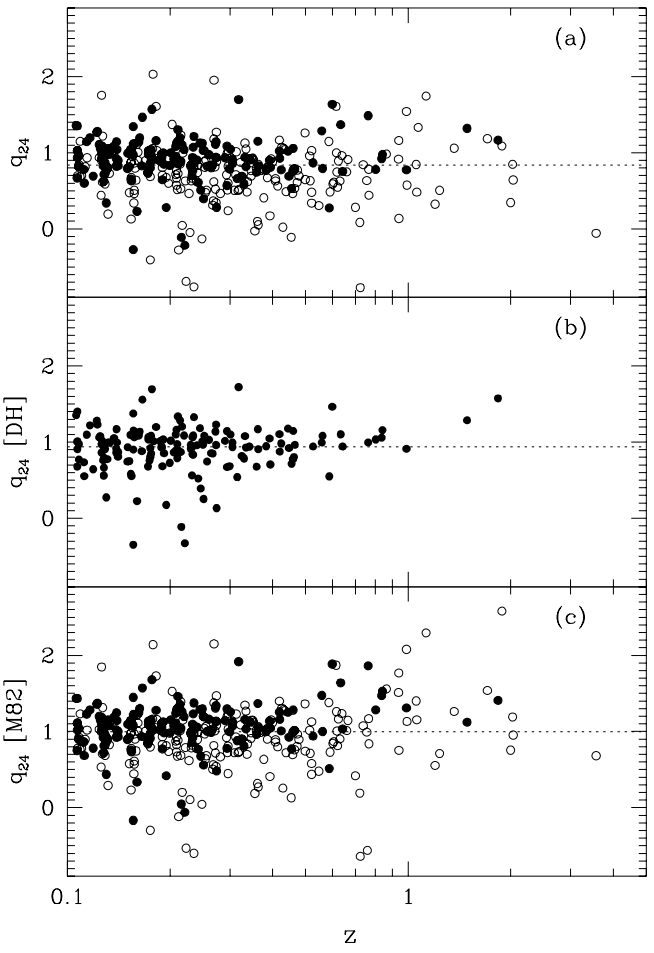

FIG. 2.—q_{24} as a function of redshift (*a*) uncorrected, (*b*) *k*-corrected using the SED-fitting method, and (*c*) corrected with an M82 template (see text).

70 μm bands, respectively. These monochromatic values for q represent the slope of the IR/radio correlation, and the dispersion about the mean q is indicative of the strength of the correlation.[10]

Figures 1*b* and 1*c* show the distribution of q_{70} points before and after the application of a *k*-correction using the SED model-fitting method. Ignoring the points below $q = 1.6$, which are associated with radio-loud AGNs, the figure shows a tight correlation between radio and 70 μm emission over a wide range of redshifts extending to $z \geq 1$.

We estimated the median and dispersion of the correlation using the biweight estimator discussed by Beers et al. (1990). This method is resistant to outliers and is robust for a broad range of non-Gaussian underlying populations. The central location (mean) value and scale (dispersion) in q_{70} before (2.16 ± 0.17) and after (2.15 ± 0.16) correction appears to be invariant with z up to 1. The slight increase in q_{70} above $z = 1$ is probably the result of small number statistics and the strong Malmquist bias, which leads to very luminous galaxies appearing in the sample at these redshifts. The highest redshift galaxies have luminosities that are of comparable to that of ULIRGs.

[10] Ideally, it would be better to measure a bolometric q, but insufficient data are available at longer wavelengths to do this reliably (see Papovich & Bell 2002). In addition, monochromatic q relationships may be of great interest for studies involving only one or two MIPS bands.

We show in Figures 2*a* and 2*b* the corresponding q diagrams for the 24 μm band. The filled circles indicate galaxies that have a measured flux at 70 μm. The dispersion in the q_{24} values at zero redshift (mean $= 0.84 \pm 0.28$) is a factor of 1.6 larger than that seen at 70 μm. A general flaring of the q_{24} distribution with z is noticeable in the uncorrected data. Figure 2*b*, which has been corrected using the SED-fitting method, has fewer points than Figure 2*a*, because the method relies on having detections at 70 μm. Since the flaring is reduced after the correction, at least part of the higher z dispersion can be attributed to variations in SED, as reflected in the statistics (mean $= 0.94 \pm 0.23$). The deviations from a constant q for the highest z galaxies may be due to Malmquist bias, which would favor very luminous ULIRGs that may show free-free absorption at radio wavelengths. Figure 2*c* contrasts the more definitive SED-fitting method with the M82-correction method applied to the complete set of 24 μm detected galaxies. The formal scatter is also slightly reduced (mean $= 1.00 \pm 0.27$), especially in the core of the distribution, although outlying points are less well corrected, presumably because M82 is not a good fit to all the SEDs (formally the M82 method reduces the scatter as well as the SED method if only the smaller number of points are considered, with the mean at 1.07 ± 0.21).

The poor 24 μm correlations at low $z < 0.2$ must reflect intrinsic variations in the IR/radio ratio within the population. Insight into this can be seen in Figure 3, which shows q_{24} as a function of the 24/70 μm color. This shows that for a given color, the galaxies have a much smaller q-dispersion. For

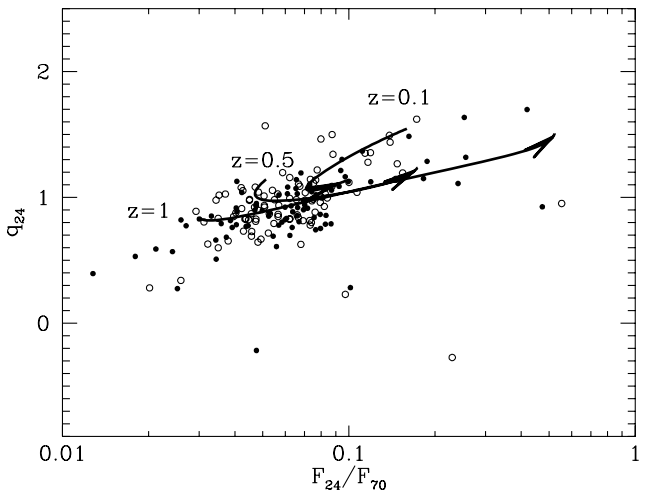

FIG. 3.—Trend of q_{24} with mid- and far-IR color. Open circles indicate galaxies with $z < 0.5$, and filled circles show galaxies with $z > +0.5$. The solid lines show the range of q parameter and colors predicted by the DH01-model SEDs for increasing values of the α parameter. The range is from $\alpha = 0.063$ to 4 (*ending with arrow*). Curves for three redshift ranges are represented.

example, it is clear that the majority of the outlying points in the q-distribution are at the extremes of the color distribution, having either very low (<0.04 S_{24}/S_{70}) or very high (>0.2) flux ratios. Note that the AGNs do not follow the clear trend with color, allowing easy separation of this population from the star-forming systems.

Also plotted in Figure 3 are the loci of the model α parameter from the SED library for three different redshift ranges. The solid lines represent the model predictions for the full range of possible α parameters represented in the model. The figure shows that the general slope and behavior of the q-versus-color diagram is extremely well represented, but the range of possible color space is too limited at present. It will be noted that many galaxies lie just outside the range of coverage of the models at low z, although at high z the models encompass more of the distribution. The consequence of the incomplete coverage of the model parameters provides an explanation for the apparent increase in q with z seen in Figure 2*b*. The model results are promising, although presently limited in scope. However, they do suggest that great improvements in the method will come with the inclusion of more steeply falling SEDs in the template library.

5. CONCLUSIONS

Observations with the *Spitzer Space Telescope* show that the slope of the 70 μm FIR/radio correlation is constant out to $z = 1$ and that the dispersion about the mean is invariant to $z = 0.5$. Further, using the higher sensitivity gained by observations at 24 μm, we show that despite the larger scatter, the MIR/radio correlation has a constant slope out to $z = 2$. In a λ-dominated universe, this implies that the "conspiracy" of finely tuned factors that have created the correlation in nearby galaxies existed in the potentially more primitive galaxies that we observe more than 8–10 Gyr in the past. Unlike some dwarf galaxies seen locally, which are unable to retain their radio-emitting plasma (and deviate from the FIR-radio correlation; Klein et al. 1984; Chi & Wolfendale 1990), these distant galaxies must be able to contain their radio-emitting plasma long enough to fall on the FIR/radio relationship. Future work will concentrate on understanding the systematic effects that lead to the increased spread in the strength of the MIR correlation, thus allowing the technique to be applied to much deeper surveys in which significant overlap of powerful submillimeter galaxy populations will be possible.

The authors wish to thank V. Charmandaris (Cornell University), D. Dale (University of Wyoming), and an anonymous referee for helpful contributions to this work.

REFERENCES

Beers, T.C., Flynn, K., & Gebhardt, K. 1990, AJ, 100, 32
Bertin, E., & Arnouts, S. 1996, A&AS, 117, 393
Carilli, C. L., & Yun, M. S. 1999, ApJ, 513, L13
Chapman, S. C., Blain, A. W., Ivison, R. J., & Smail, I. R. 2003, Nature, 422, 695
Chi, X., & Wolfendale, A. W. 1990, MNRAS, 245, 101
Cohen, J., et al. 2000, ApJ, 538, 29
Condon, J. J., & Broderick, J. J. 1986, AJ, 92, 94
Condon, J. J., Condon, M. A., Gisler, G., & Puschell, J. 1982, ApJ, 252, 102
Condon, J. J., Cotton, W. D., Yin, Q. F., Shupe, D. L., Storrie-Lombardi, L. J., Helou, G., Soifer, B. T., & Werner, M. W. 2003, AJ, 125, 2411
Dale, D. A., Helou, G., Contursi, A., Silbermann, N. A., & Kolhatkar, S. 2001, ApJ, 549, 215 (DH01)
de Jong, T., Klein, U., Wielebinski, R., & Wunderlich, E. 1985, A&A, 147, L6
Dickey, J. M., & Salpeter, E. E. 1984, ApJ, 284, 461
Diolaiti, E., Bendinelli, O., Bonaccini, D., Close, L., Currie, D., & Parmeggiani, G. 2000, A&AS, 147, 335
Elbaz, D., Cesarsky, C. J., Chanial, P., Aussel, H., Franceschini, A., Fadda, D., & Chary, R. R. 2002, A&A, 384, 848
Fadda, D., Jannuzi, B., Ford, A., & Storrie-Lombardi, L. J. 2004, AJ, 128, 1
Fadda, D., et al. 2002, A&A, 383, 838
Fazio, G. G., et. al. 2004, ApJS, 154, 10
Fitt, A. J., Alexander, P., & Cox, M. J. 1988, MNRAS, 233, 907
Frayer, D. T., et al. 1999, ApJ, 514, L13
Garrett, M. 2002, A&A, 384, L19
Gruppioni, C., et al. 2003, MNRAS, 341, L1
Helou, G., Soifer, B. T., & Rowan-Robinson, M. 1985, ApJ, 298, L7
Hogg, D. W., Baldry, I. K., Blanton, M. R., & Eisenstein, D. J. 2002, preprint (astro-ph/0210394)
Hummel, E., Davies, R. D., Wolstencroft, R. D., van der Hulst, J. M., & Pedlar, A. 1988, A&A, 199, 91
Ivison, R. J., Smail, I., Le Borgne, J.-F., Blain, A. W., Kneib, J.-P., Bezecourt, J., Kerr, T. H., & Davies, J. K. 1998, MNRAS, 298, 583
Ivison, R. J., et al. 2002, MNRAS, 337, 1
Klein, U., Wielebinski, R., Thuan, T. X. 1984, A&A, 141, 241
Papovich, C., & Bell, E. F. 2002, ApJ, 579, L1
Rickard, L. J., & Harvey, P. M. 1984, AJ, 89, 1520
Rieke, M. J., et al. 2004, ApJS, 154, 25
van der Kruit, P. C. 1973, A&A, 29, 263
Weedman, D. W. 1986, Quasar Astronomy (Cambridge: Cambridge Univ. Press), 61
Wunderlich, E., Klein, U., & Wielebinski, R. 1987, A&AS, 69, 487